Smart Structures and Systems, *Vol. 28, No. 2 (2021) 153-165*
https://doi.org/10.12989/sss.2021.28.2.153

Modifications on F^2MC tubes as passive tunable vibration absorbers

Shiren O. Muhammad* and Nazhad A. Hussain [a]

Department of Mechanical and Mechatronics Engineering, Salahaddin University - Erbil, Erbil,44002, Kurdistan Region, Iraq

(*Received August 15, 2019, Revised April 6, 2021, Accepted April 11, 2021*)

Abstract. This paper presents new parameters for damping improvement in F^2MC tubes performance as tunable vibration absorbers. They offer very good performance with environments having susceptibility to high frequency vibration noise. This study highlights the behavior of changing some parameters of F^2MC tubes which never have been studied before. These parameters include thickness ratio between each two respective layers and fluid type that the tubes are filled with. In this paper the beam governing equations with the tube's stress analyses equations are solved for finding the combined system's response by MATLAB® software function solvers. To ensure accuracy of modifications, validations have been proposed by performing illustrative examples and comparing the results with the existing data available in literature. The results showed improvements of F^2MC tubes performance 20% over previous studies achievements by studying the thickness ratio, and another 12.82% can be added by using glycerin instead of water under the same conditions. Finally, the reduction of 34.34 dB in first mode amplitude of vibration was achieved in the beam's frequency response function plot.

Keywords: damping; F^2MC tubes; first mode shape; frequency response function plot; passive vibration absorbers; vibration control

1. Introduction

1.1 Problem background

The problem of reducing vibrations in machines and structures has been under investigation for many years. , the first studies late back to Roberson (1952), who studied the synthesis of a nonlinear dynamic vibration absorber by using both of duffing iteration method and electronic drential analyzer.

Additionally, Nonlinear vibration absorber has been implemented on a flexible structure. The system was composed of piezoceramic patch integrated on the structure. The results were obtained numerically, and the validations has been done by using strain gauges. The stability analysis was investigated for both transient and steady state performance of the system through numerical simulations, (Oueini *et al*. 1998). A detailed investigation on the response of nonlinear energy sink on a linear oscillator with external harmonic forcing has been presented through numerical and experimental studies (Starosvetsky and Gendelman 2008).

The delayed feedback control is one of the effective methods to suppress vertical vibrations on the structures (Zhao and Xu 2007).

A methodology for tuning a nonlinear absorber coupled with a nonlinear oscillator is numerically simulated for both nonlinear and linear elastic terms. As a result, the system possessed energy-invariant straight modal curves (Viguié and Kerschen 2009).

Active vibration control usually produces high damping force but they are unstable (Nakahara and Fujimoto 2011, Takács *et al*. 2016). Semi-active controllers outcome high function faster than active vibration controllers (Itoh *et al*. 2011). Input shaping technique is a passive control method which reduces vibrations with high efficiency in linear time invariant systems (Yun *et al*. 2008). Whereas, Fluidic Flexible Matrix Composite (F^2MC) are one of the most effective systems that can be easily integrated to the structures, and have ability to control vibrations of nonlinear time variant systems.

F^2MC tubes are light weight composite tubes, consist of a high anisotropic laminate shell with reinforcements of $\pm\alpha^o$ with respect to longitudinal axis. Over the last thirteen years, several studies have dealt with their parametric studies for various applications, these included: Their ability to maintain actuation (Shan *et al*. 2006, Zhang *et al*. 2010, Zhu *et al*. 2011); variable volume and stiffness (Philen *et al*. 2006, Philen 2008); as tunable modulus structures (Philen 2010); for vibration absorption (Lotfi-Gaskarimahalle *et al*. 2009, Zhu *et al*. 2014b), for vibration isolation (Philen 2012), and damping treatment (Lotfi-Gaskarimahallea *et al*. 2008, Zhu *et al*. 2013b, 2015) in vibration control applications.

1.2 Formulation of the problem of interest for this investigation

In the past ten years, Zhu *et al*. (2014a) designed a three-layered F^2MC tubes, and examined their vibration

*Corresponding author,
M.Sc., Ph.D. Student, Assistant Lecturer,
E-mail: shireen.muhammad@su.edu.krd
[a] Ph.D.

http://www.techno-press.org/?journal=sss&subpage=7
ISSN: 1738-1584 (Print), 1738-1991 (Online)

absorbing capacity by using two fluidic circuits. In the first circuit orifice was used, and the other circuit used inertia track and accumulator. The reduction amplitude of vibration in the first mode shape in both circuits was recorded as 20 dB and 27 dB respectively. Even though, Zhu *et al*. (2014b) F^2MC tubes with the same design had been integrated on a cantilever beam. Here, the tube attachment location with flow control through inertia truck had been studied. The reduction of 35 dB in amplitude of first mode shape was obtained. Krott *et al*. (2015) constructed F^2MC tube for a damped fluidic absorber on a small-scale tail-boom experimentally. The characterized parameters were bladder materials and wall thickness. Simulations show that thin and soft F^2MC tube bladders maximize vibration absorption. Their results showed a 17.2 dB reduction in first vertical bending mode of tail-boom by using 0.8 mm thick rubber bladder and stainless-steel mesh. The above studies prove the ability of using F^2MC tubes as tunned vibration absorbers, but modifications are needed to indicate the parameters may lead to better results. To clarify more, the following parameters has not been studied as tuned vibration absorbers: studying the thickness of layers as a ratio of sizes for two respective layers; optimization of the points which the tubes integrated on the beam; comparing the usage of different fluids inside the tubes.

1.3 Literature survey

In the development of composite materials there has been a lot of research that creating new possibilities for making innovative structures. Different capabilities have been recently seen with filament wound composite F^2MC tubes comprising stiff fibres such as carbon embedded in a high flexible elastomeric matrix like polyurethane. Their ability as a variable volume structures were discovered by flow control valve (Philen *et al*. 2006), which performs variable stiffness skin with high out of plane stiffness. Additionally, by changing the fibre orientation and base material of these tubes the nearly endless stiffness ratios can have been obtained. Likewise, by changing the internal pressure, the tube behaved like an actuator (Shan *et al.* 2006). There had been studies showed the F^2MC tube's same advantages as McKibben muscles (Philen *et al*. 2007). A three-dimensional analytical model was evolved to describe the axial stiffness of a single F^2MC tube, and wide range of modulus ratios was attained by embedding multiple tubes side by side in a soft matrix (Shan *et al.* 2009). Tailoring geometry and material properties of F^2MC tubes made them easy to be used in different applications.

Recently, F^2MC tube technology got successful achievements in variety of aerodynamic applications for the purpose of controlling vibrations, such as in rotor crafts (Kurczewski *et al*. 2012), vibration isolation in helicopter rotor craft pitch links (Scarborough 2014), and vibration absorbers in tail boom helicopters (Kirn *et al*. 2011, Miura *et al*. 2015, Krott *et al*. 2015). F^2MC tubes can be made from multi-layer tubes, changing the number of layers or material type of them can easily change the behavior of these tubes in areas of applications. The absorbing capacity of two layered F^2MC tubes under different fluid flow coefficients by variating orifice size had been studied. The results over weighted large orifices on smaller once for better damping (Lotfi-Gaskarimahalle *et al*. 2009).

1.4 Scope and contribution of this study

The main contribution of this study is to develop a passive tunned vibration absorber by using F^2MC tubes. Nowadays, cantilever structures are used in different studies because of their usage in verity of applications. To exemplify this: (Wang and Shi 2015) considered each of sensor, driving displacement and blocking force models for studying static performance of fully covered a piezoelectric bilayer cantilever with electrodes on the upper and lower surfaces; (Loktionov 2017) investigated a model for determining support moment of a cantilever beam; (Usharani 2017) designed energy harvester system on a cantilever beam with variable overhang length, by using a new technique for increasing its operation frequency; (Casas-Ramos and Sandoval-Romero 2017) used a cantilever beam for presenting their experimental results of a vibration sensor to generate axial strain in fiber grating in-line with its vertical axis; and Ghodsi (2019) made investigations on cantilevered beam energy harvester system.

One of the potential limitations of F^2MC tubes as vibration absorbers is not including studying the thickness of layers of these tubes on the system performance as vibration absorbers. Additionally, the previously done studies include examining these tubes filled only with water. Despite of the interest of changing the type of fluid inside F^2MC tubes, no one to the best of our knowledge has been focused on it. In this paper three different fluids: gasoline, glycerin and mercury has been used as working fluids for modified F^2MC tubes. Then the tube's performance filled with the mentioned fluids has been studied.

1.5 Organization of this study

In this paper the qualitative tuning methodology for such a vibration absorber has been proposed. The paper organized as follow: in Section 2 mathematical modelling of the F^2MC tube-beam system has been developed. In Section 3 the validations of derived model have been proposed. Then both of parametric studies and discussion have been presented in Section 4 under a title of result analysis. Then the conclusions of the present study are summarized in Section 5.

This study examined the efficiency of these tubes for vibration control when gasoline, glycerin, and mercury rather than water has been tested. The analytical model of compound structure of F^2MC tubes integrated on cantilever beam solved through MATLAB® software function solvers, to ensure accuracy of modifications, validations have been proposed by performing illustrative examples and comparing the results with the existing data available in literature. Then, it has been applied to find the complete systems transfer function as Frequency Response Function (FRF) plot. In this study layer thickness ratio as a new parametric study has been optimized, layer thickness ratio is the ratio of thickness between any two respective layers of the tube. Additionally, the whole system's FRF was studied to find best clamping points through examining different bonding positions for F^2MC tubes on the beam. Finally, different flow coefficients were examined to find the best flow coefficient that able to introduce maximum damping to the beam.

2. Governing equations

The study deals with two F^2MC tubes, controlled by orifice and accumulator, filled with fluid, clamped on the cantilever beam. The F^2MC tubes used in this study are consist of three layers; two liner layers surrounding with one composite laminate layer in the middle. Polyurethane was selected as liner layer material with E = 11 Mpa, and v = 0.498, whereas, the middle layer was selected as composite fibre reinforced laminate, with polyacrylonitrile based carbon fiber as a matrix material. Because FMC tube's tuning is achieved by tailoring material type (Philen *et al*. 2007), which might have effect on the damping resonance frequency, as well as the damping peak amplitudes. The transversely orthotropic sublayers of ±α with fiber orientation angle α = 17°. A uniform cantilever beam made from aluminum, with rectangular cross section, and an applied point load (F) was chosen for this study. Then a system of F^2MC tubes connected on the beam by bonding in two points ($x1$ and $x2$) from the two ends of the F^2MC system. The force (F) tends to stretch the system of F^2MC tubes longitudinally by an axial force F_t, resulted in formulation of moment (M) as

$$M = F_t \times d \tag{1}$$

where (d) is the distance between the neutral axis of the beam and the centre line of the beam.

2.1 Beam equations

Beam governing equations are found depending on Euler Bernoulli theory for three domains of the beam as

$$Y = \begin{cases} Y1(x,s) = A1 sin\beta x + A2 cos\beta x + A3 sinh\beta x + A4 cosh\beta x, & \text{for } x\epsilon(0, x_1) \\ Y2(x,s) = B1 sin\beta x + B2 cos\beta x + B3 sinh\beta x + B4 cosh\beta x, & \text{for } x\epsilon(x_1, x_2) \\ Y3(x,s) = C1 sin\beta x + C2 cos\beta x + C3 sinh\beta x + C4 cosh\beta x, & \text{for } x\epsilon(x_2, L) \end{cases} \tag{2}$$

Where Y is come from the general equation,

$$m\frac{d^2y}{dt^2} + B\frac{dy}{dt} + EI\frac{d^4y}{dx^4} = 0 \quad \text{for} \quad x \in (0, L). \tag{3}$$

where m, B, E, and I are mass, damping coefficient, modulus of elasticity and moment of inertia of the beam respectively. The beams geometry and material type are detailed in Table 1. The mass of the beam can be calculated through beam's material density and cross-sectional area by

$$m = \rho \times b \times h \tag{4}$$

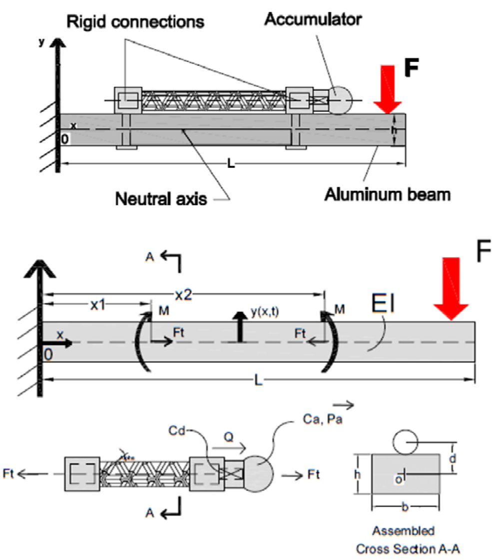

Fig. 1 F^2MC tube Integrated on cantilever beam: (A) General view; (B) Explaining forces, moments and attaching tube locations

solving Eq. (3) in Laplace transform with zero initial conditions led to

$$\frac{d^4Y}{dx^4} - \beta^4 Y(x) = 0 \tag{5}$$

with

$$\beta^4 = \frac{s^2 m + sB}{EI} \tag{6}$$

And, the constants An, Bn and Cn for (n = 1, 2, 3, 4) are found by using beam boundary conditions, moment balance, and continuity equations (Gere 2004) as below

At $x = 0$ the beam is clamped, so

$$W1(0,s) = W1'(0,s) = 0.$$

$At\ x = x1$, taking the moment balance yields

$$EI\big(W2''(x1,s) - W1''(x1,s)\big) = M(s).$$

where $M(s) = \mathscr{L}(M(t))$, and applying continuity

$$W1(x1,s) = W2(x1,s),$$
$$W1'(x1,s) = W2'(x1,s),$$
$$W1'''(x1,s) = W2'''(x1,s).$$

In the same way at $x = x2$ a moment balance gives

$$EI\big(W2''(x2,s) - W3''(x2,s)\big) = M(s),$$

where $M(s) = \mathcal{L}(M(t))$, and applying continuity

Table 1 Geometry of F²MC tubes with fluid's physical properties and material type of the beam

Fibre reinforced layer (middle layers) Longitudinal modulus of elasticity	E_{11}	40 GPa
Transverse modulus of elasticity	E_{22}	1.8 MPa
Poison's ratios	ν_{12}	0.33
	ν_{23}	0.39
Modulus of rigidity	G_{12}	1.4 MPa
Fibre angle	α	±27°
Liner layer (inner and outer) elastic modulus	E_o	11 MPa
Poisons ratio	ν_o	0.498
F²MC tube's inner layer radius	c_1	0.54, (0.36-0.81) mm
Middle layer radius	c_2	0.9 mm
Outer layer internal radius	c_3	1.28, $c_3 > c_1$, (1-3) mm
Outer layer external radius	c_4	1.406, $c_4 > c_3$, (1.1-10) mm
F²MC tube length	L_{FMC}	$x_1 - x_2$
First bonding point distance from the fixed end	x_1	0
Last bonding point distance from the fixed end	x_2	150 mm
Number of F²MC tubes	N	2
Centre to centre distance	d	9 mm
Accumulator capacitance	C_a	1.5×10^{-9} m³/pa
Flow coefficients	C_d	$2 \times 10^{-13}, (10^{-15} - 10^{-7})$ m³/s pa
Beam material (Aluminum)	E	70 Gpa
Damping constant	B	0.2 Ns/m
Density	ρ	2700 kg/m³
Cross sectional height	h	1.6 mm
Cross sectional width	b	26 mm
Length of the beam	L	310 mm

$$W2(x2, s) = W3(x2, s),$$
$$W2'(x2, s) = W3'(x2, s),$$
$$W2'''(x2, s) = W3'''(x2, s).$$

At ($x = L$) the tip shear and moment and balances give

$$EIW3'''(L, s) = F(s),$$
$$EIW3''(L, s) = 0,$$
$$\text{where} \quad F(s) = \mathcal{L}(F(t)).$$

As a result, twelve equations are obtained as a function of the constants all twelve constants.

2.2 F²MC tube equations

The layers of the tubes are coaxial and perfectly bonded. So, they can be assumed as hollow wires bonded together, with a radii of c_1, c_2, c_3 and c_4 from inside to outside, respectively (Fig. 2). The axial force acting on each tube is calculated through force balance on each layer

$$T = T_1 + T_2 + T_3 \tag{7}$$

where T_1, T_2 and T_3 are calculated by stress, and strain equations in r, θ, and z coordinates for each layer respectively. In the same time this force can be found by summation of axial forces on each tube and fluid force inside them

$$T = \frac{Ft}{N} + p_o \pi c_1^2 \tag{8}$$

where (p_o) is fluid pressure inside the tubes and (N) is the number of tubes. For the Inner and outer layers, liner material selected, so they follow an infinite long isotropic

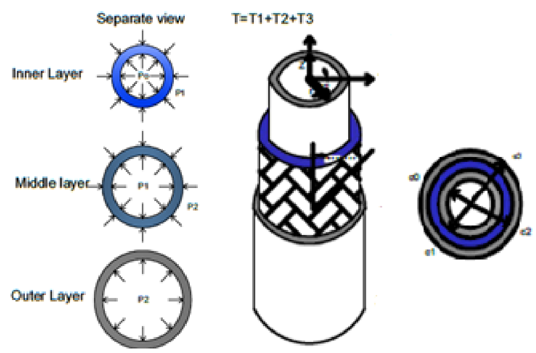

Fig. 2 Details of load, pressures, and dimensions of F²MC tubes

cylinder, the stress and strain equations regarding to the force and pressures acting on each layer (Boresi *et al.* 1993). The Inner layer equations

$$\sigma_r^i = \frac{p_o c_1^2 - p_1 c_2^2}{c_2^2 - c_1^2} - \frac{c_1^2 c_2^2 (p_o - p_1)}{c^2(c_2^2 - c_1^2)}, \tag{9}$$

$$\sigma_\theta^i = \frac{p_o c_1^2 - p_1 c_2^2}{c_2^2 - c_1^2} + \frac{c_1^2 c_2^2 (p_o - p_1)}{c^2(c_2^2 - c_1^2)}, \tag{10}$$

$$\sigma_z^i = \frac{T_1}{\pi(c_2^2 - c_1^2)}, \tag{11}$$

The strains in each direction can be obtained by using Hooke's law

$$\varepsilon_r^i = \frac{1}{E_o}\left[\sigma_r^i - v_o\left(\sigma_\theta^i + \sigma_z^i\right)\right], \tag{12}$$

$$\varepsilon_\theta^i = \frac{1}{E_o}\left[\sigma_\theta^i - v_o\left(\sigma_r^i + \sigma_z^i\right)\right], \tag{13}$$

$$\varepsilon_z^o = \frac{1}{E_o}\left[\sigma_z^i - v_o\left(\sigma_\theta^i + \sigma_r^i\right)\right], \tag{14}$$

where p_2 is the pressure that middle layer formulates on the surface of inner layer from outside, T_1 is a force that acts on the inner layer. In the same way, the outer layer equations are

$$\sigma_r^o = \frac{p_2 c_3^2 - p_3 c_4^2}{c_4^2 - c_3^2} - \frac{c_3^2 c_4^2 (p_2 - p_3)}{c^2(c_4^2 - c_3^2)}, \tag{15}$$

$$\sigma_\theta^o = \frac{p_2 c_3^2 - p_3 c_4^2}{c_4^2 - c_3^2} + \frac{c_3^2 c_4^2 (p_2 - p_3)}{c^2(c_4^2 - c_3^2)}, \tag{16}$$

$$\sigma_z^o = \frac{T_3}{\pi(c_4^2 - c_3^2)}, \tag{17}$$

The strains in each direction can be obtained by using Hooke's law

$$\varepsilon_r^o = \frac{1}{E_o}[\sigma_r^o - v_o(\sigma_\theta^o + \sigma_z^o)], \tag{18}$$

$$\varepsilon_\theta^o = \frac{1}{E_o}[\sigma_\theta^o - v_o(\sigma_r^o + \sigma_z^o)], \tag{19}$$

$$\varepsilon_z^o = \frac{1}{E_o}[\sigma_z^o - v_o(\sigma_\theta^o + \sigma_r^o)], \tag{20}$$

with p_2 is the pressure that formulated by middle layer acts on the internal surface of outer layer, p_3 is the air pressure outside the tube, it has been neglected (p_3 = 0), T_3 is a force that acts on the outer layer. And the Young's modulus of elasticity (E), Poisson's ratio (v) for inner and outer was chosen to be polyurethane.

The middle layer is made from fibre reinforced composite layers, with an internal surface pressure (p_1) and external surface pressure (p_2). The axial force is T_2. The stress equations follow Lekhnitskii's elasticity solution for homogenous orthotropic cylinders (Lekhnitskii 1977) as

$$\sigma_r^m = \frac{p_1 a^{k+1} - p_2}{1 - a^{2k}} \mu^{k-1} + \frac{p_2 a^{k-1} - p_1}{1 - a^{2k}} a^{k+1} \mu^{k-1} + AhK_1, \tag{21}$$

$$\sigma_\theta^m = \frac{p_1 a^{k+1} - p_2}{1 - a^{2k}} k\mu^{k-1} + \frac{p_2 a^{k-1} - p_1}{1 - a^{2k}} k a^{k+1} \mu^{k-1} + AhK_2, \tag{22}$$

$$\sigma_z^m = A - \frac{1}{b_{33}}(b_{13}\sigma_r^m + b_{23}\sigma_\theta^m), \tag{23}$$

where r, θ and z indicate radial, hoop and axial directions (Fig. 3)

$$a = \frac{c_2}{c_3}, \tag{24}$$

$$\mu = \frac{c}{c_3}, \tag{25}$$

$$k = \sqrt{\frac{\beta_{11}}{\beta_{22}}}, \tag{26}$$

$$h = \frac{b_{23} - b_{13}}{\beta_{11} - \beta_{22}}, \tag{27}$$

$$\beta_{11} = b_{11} - \frac{b_{13}}{b_{33}}, \tag{28}$$

$$\beta_{22} = b_{22} - \frac{b_{23}^2}{b_{33}}, \tag{29}$$

$$K_1 = 1 - \frac{1 - a^{k+1}}{1 - a^{2k}} \mu^{k-1} - \frac{1 - a^{k-1}}{1 - a^{2k}} a^{k+1} \mu^{k-1}, \tag{30}$$

$$K_2 = 1 - \frac{1 - a^{k+1}}{1 - a^{2k}} k\mu^{k-1} + \frac{1 - a^{k-1}}{1 - a^{2k}} k a^{k+1} \mu^{-k-1}, \tag{30}$$

The b_{ij} terms are three-dimensional effective compliance constants found from the homogenous properties of the inner layer in the cylindrical coordinate system (Sun and Li 1988, Bakaiyan *et al.* 2009). For the transversely orthotropic unidirectional reinforced $(+\alpha)$ and $(-\alpha)$ sub-layers; they have five independent elastic constants: longitudinal and transverse modulus of elasticity $E11$, $E22$, Poisson's ratio ν_{12} and ν_{23} and longitudinal shear modulus of elasticity G_{12}. And the axial force T_2 can be calculated by integrating stress in the axial direction as

$$T_2 = 2\pi \int_{c_2}^{c_3} \sigma_z^m c\,dc, \tag{32}$$

The parameter A is found by solving Eqs. (21), (22), (23), and (32) as a function of $(T_2, p_1 \text{ and } p_2)$. The strain distributions for the inner composite layer are

$$\varepsilon_r^m = b_{11}\sigma_r^m + b_{12}\sigma_\theta^m + b_{13}\sigma_z^m, \tag{33}$$

$$\varepsilon_\theta^m = b_{12}\sigma_r^m + b_{22}\sigma_\theta^m + b_{23}\sigma_z^m, \tag{34}$$

$$\varepsilon_z^m = b_{13}\sigma_r^m + b_{23}\sigma_\theta^m + b_{33}\sigma_z^m, \tag{35}$$

The stress and strain equations from all layers are solved together by assuming plain stain solution and perfect bonding, the tubes extend equally in axial direction and on the interface between layers. So, both axial and tangential strains are identical. In the other words

$$\varepsilon_z^i = \varepsilon_z^m, \tag{36}$$

$$\varepsilon_z^m = \varepsilon_z^o. \tag{37}$$

$$\varepsilon_\theta^i\big|_{c=c_2} = \varepsilon_\theta^m|_{c=c_2} \tag{38}$$

$$\varepsilon_\theta^m|_{c=c_3} = \varepsilon_\theta^o|_{c=c_3} \tag{39}$$

Following the above assumptions with Eq. (8), and substituting geometry and material properties, the axial and tangential strains are solved as a function of fluid internal pressure (p_o) and axial force T, as

$$\varepsilon_\theta|_{r=c_1} = \emptyset_1 T + \emptyset_2 p_0 \tag{40}$$

and

$$\varepsilon_z = \emptyset_3 T + \emptyset_4 p_0 \tag{41}$$

where $\emptyset_1$, $\emptyset_2$, $\emptyset_3$ and $\emptyset_4$ are constants representing the geometry and material properties of the F^{2}MC tubes.

2.3 Fluid behavior

The study focuses on studying F^{2}MC tubes working fluid behavior only when the control valve is closed. It is assumed that the tube is filled with fluid, is tight with no differential pressure with the bulk modulus (B_f) and volume of (V_i). When the force (F) is applied, the volume of the F^{2}MC tubes changes by the amount of (ΔV_f) with the formation of (F_t). Depending on the volume change, the fluid differential pressure changes from zero to (p_o). This can be expressed as

$$\left(\frac{\Delta V_f}{V_i}\right) B_f = -P_o, \tag{42}$$

but the volume change of F^{2}MC tube is defined as

$$\Delta V = V - V_i, \tag{43}$$

where

$$V = \pi\left[(1 + \varepsilon_\theta|_{r=c_1})c_1\right]^2 \tag{44}$$

$$V_i = \pi a_0^2 (x2 - x1), \tag{45}$$

hen, the volume ratio can be written as

$$\frac{\Delta V}{V_i} = \frac{V_i - V}{V_i} \equiv \varepsilon_z + 2\varepsilon_\theta|_{r=c_1} \tag{46}$$

The amount of fluid volume that pumped out of the system of F^{2}MC tubes, which is composed of (N = 2) tubes connected in parallel, assumed as the fluid volume flow rate and expressed as

$$Q_V = -N(\Delta V - \Delta V_f). \tag{47}$$

by substituting each of ΔV_f and ΔV from Equations (42) and (43) respectively, yields to

$$Q_V = NF_Q\frac{dT}{dt} + NG_Q\frac{dp_0}{dt} \tag{48}$$

where

$$G_Q = -(\emptyset_1 + 2\emptyset_3)V_i \tag{49}$$

$$F_Q = -\left(\emptyset_2 + 2\emptyset_4 + \frac{1}{B_f}\right)V_i \tag{50}$$

The fluid volume flow rate also balances the change in fluid pressure inside the orifice and accumulator by

$$Q_V = C_d(p_0 - p_A) \tag{51}$$

and

$$Q_V = C_a\frac{dp_A}{dt} \tag{52}$$

where (p_A) is the internal pressure of the accumulator, (C_d) the flow coefficient and (C_a) is the accumulator capacity.

2.4 Solution of system governing equations

The transfer function of the F^{2}MC system is determined as a ratio of the axial strain to the axial force by solving Eqs. (8), (41), (48), (51) and (52) in the Laplace domain with zero initial conditions as follows

$$\varepsilon_z(s) = G_p(s)F_t(s), \tag{53}$$

where

$$G_p(s) = \frac{(c_a s + c_d)(\emptyset_3 F_Q - \emptyset_4 G_Q) - \theta_3 c_a c_d / N}{N(c_a s + c_d)(F_Q + \pi c_1^2 G_Q) - c_a c_d} \tag{54}$$

As required by Lekhnitskii's theory of elasticity (Lekhnitskii 1977), the strip stretches uniformly in an axial direction, and the total F^{2}MC tube elongation can be calculated as

$$\Delta L(s) = L_{FMC}\varepsilon_z(s) = -d\left(\frac{dY_2(s)}{dx2} - \frac{dY_2(s)}{dx1}\right), \tag{55}$$

Substituting (F_t) and (d) in Eq. (53) and (55) into Eq.

(1) then solving for moment (M), yields the following equation

$$M(s) = \frac{1}{M(s)}\left[\frac{dY_2(s)}{dx2} - \frac{dY_2(s)}{dx1}\right], \tag{56}$$

where

$$N(s) = \frac{L_{FMC}}{d^2} G_p(s) \tag{57}$$

Now, substituting Eq. (56) into the constants equations which is depend on beam boundary conditions, moment and continuity equations and the following expression can be obtained

$$Jw = bF(s), \tag{58}$$

where

$$J = \begin{bmatrix} 0 & 1 & 0 & 1 & 0 & 0 & 0 & 0 & 0 & 0 & 0 & 0 \\ 1 & 0 & 1 & 0 & 0 & 0 & 0 & 0 & 0 & 0 & 0 & 0 \\ J_{31} & J_{32} & J_{33} & J_{34} & J_{35} & J_{36} & J_{37} & J_{38} & 0 & 0 & 0 & 0 \\ 0 & 0 & 0 & 0 & J_{45} & J_{46} & J_{47} & J_{48} & J_{49} & J_{410} & J_{411} & J_{412} \\ 0 & 0 & 0 & 0 & 0 & 0 & 0 & 0 & -C\beta L & S\beta L & Ch\beta L & Sh\beta L \\ 0 & 0 & 0 & 0 & 0 & 0 & 0 & 0 & -S\beta L & -C\beta L & Sh\beta L & Ch\beta L \\ S\beta x1 & C\beta x1 & Sh\beta x1 & Ch\beta x1 & \text{-}S\beta x1 & -C\beta x1 & -Sh\beta x1 & -Ch\beta x1 & 0 & 0 & 0 & 0 \\ C\beta x1 & -S\beta x1 & \mathrm{Ch}\beta x1 & Sh\beta x1 & C\beta x1 & S\beta x1 & -Ch\beta x1 & -Sh\beta x1 & 0 & 0 & 0 & 0 \\ -C\beta x1 & S\beta x1 & Ch\beta x1 & Sh\beta x1 & C\beta x1 & -S\beta x1 & -Ch\beta x1 & -Sh\beta x1 & 0 & 0 & 0 & 0 \\ 0 & 0 & 0 & 0 & S\beta x2 & C\beta x2 & Sh\beta x2 & Ch\beta x2 & -S\beta x2 & -C\beta x2 & -Sh\beta x2 & -Ch\beta x2 \\ 0 & 0 & 0 & 0 & C\beta x2 & -S\beta x2 & Ch\beta x2 & Sh\beta x2 & -C\beta x2 & S\beta x2 & -Ch\beta x2 & -Sh\beta x2 \\ 0 & 0 & 0 & 0 & -C\beta x2 & S\beta x2 & Ch\beta x2 & Sh\beta x2 & C\beta x2 & -S\beta x2 & -Ch\beta x2 & -Sh\beta x2 \end{bmatrix}$$

$$w = \begin{bmatrix} A1 \\ A2 \\ A3 \\ A4 \\ B1 \\ B2 \\ B3 \\ B4 \\ C1 \\ C2 \\ C3 \\ C4 \end{bmatrix} \qquad b = \begin{bmatrix} 0 \\ 0 \\ 0 \\ 0 \\ \frac{1}{EI\beta^3} \\ 0 \\ 0 \\ 0 \\ 0 \\ 0 \\ 0 \\ 0 \end{bmatrix} \tag{59}$$

and

where S, C, Sh, Ch, and N are sin, cos, sinh, cosh, and $N(s)$ respectively.

The total deflection at the free end of the beam is

$$\begin{aligned} Y(L,s) = {} & C1 \sin\beta L + C2 \cos\beta L \\ & + C3 \sinh\beta L + C4 \cosh\beta L \end{aligned} \tag{60}$$

and the overall transfer function of the F^2MC structure is

$$\frac{Y(L,s)}{F(s)} = a_w J^{-1} b = H(s) \tag{61}$$

with $a_w = [0 \;\; 0 \;\; 0 \;\; 0 \;\; 0 \;\; 0 \;\; 0 \;\; 0 \;\; \sin\beta L \;\; \cos\beta L \;\; \sinh\beta L \;\; \cosh\beta L]$, and the FRF is represented by $|H(j\omega)|$.

3. Model validation

At first, some illustrative examples are performed and the results are compared with the existing data available in the literature to demonstrate the accuracy of the present model. As a first example, comparisons are made between the FRF plot obtained from the previous studies and those obtained in literatures; Zhu *et al.* (2013a, 2014a and 2015) for F^2MC tubes integrated on the cantilever beam (Fig. 3). As can be seen, the present results are in well agreement with similar ones available in previous studies (Zhu *et al.* 2015), which had been agreed with their experimental validations. This agreement improved the proposal of a new model strong enough to be used for future studies.

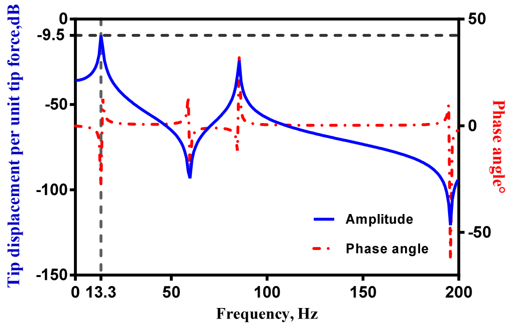

Fig. 3 Frequency response plot (Magnitude and phase angle) for (Zhu *et al.* 2015) model for comparison purpose

4. Result analysis

The present study modified the F^2MC tubes' performance for damping improvement of a cantilever beam by variation of three parameters: tube layer thickness ratio (R_1, R_2 and R_3); places where the tubes integrated on the beam (x_1, x_2); and examination of different fluids with variation of flow coefficient (c_d). The details of studies are explained below:

4.1 Modification on the tube's thickness of layers

In this part of the study, the effect of changing the thickness of layers of the F^{2}MC tubes from inside to outside (R_1, R_2, and R_3) for the fixed value of middle layer internal radius ($c_2 = 0.9$ mm) has been calculated. For this issue the new calculated thickness values have been found depending on the below relations

$$\begin{aligned} c_1 &= R_1 c_2, \\ c_3 &= c_2/R_2, \\ c_4 &= c_3/R_3. \end{aligned} \tag{62}$$

In this case study for all layers, the values of $R_i = \{0.3, 0.4, 0.5, 0.6, 0.7, 0.8, 1\}$, for $i = \{1, 2, 3\}$, had taken. In such a way that for each value of R$_1$ all possible values of R_2 and R_3 were examined. As a result, a total of 245 cases were plotted. For each case the thickness of only one layer has changed, and the others kept constant. In such a way that for each possible value of c_1; all values of c_2 and c_3 were examined. For result organization, the first three Resonance Amplitudes (RA) of the system response has been considered. The value of thickness ratio (*Ri*) that gave minimum RA with smallest resonance frequency was chosen to fix the radii of modified F^{2}MC tubes. The optimization process of thickness ratios gave the system to be examined under different values of internal to external radius of the tubes, c_2 had kept constant, whereas c_1 = (0.27, 0.36, 0.45, 0.54, 0.63, 0.72 and 0.81 mm), c_3 = (3, 2.25, 1.8, 1.5, 1.28, 1.125, and 1 mm), c_4 = (10, 5.625, 3.6, 2.5, 1.84, 1.406, and 1.111 mm).

Figs. 4 and 5 shows the optimization results of studied thicknesses by several plots of First Mode Shape (FMS) amplitude as a function of c1 for different values of R_3 and R_4. It can be found that, the radius of each layer has effect on changing the amplitudes of vibration. The maximum fall in amplitude of vibration for the overall beam system has been obtained with inner radius of 0.54 mm. further increasing this value showed a rose of amplitude again.

In contrast, decreasing thickness of each layer to some limit has positive effect on damping of the system. The minimum recorded amplitude in this study is -14.8638 dB, while the maximum amplitude is -13.556 dB, and the overall reduction in amplitude of FMS is 1.31 dB with c_1 = 0.54 mm ($R_1 = 0.6, R_2 = 0.7$ and $R_3 = 0.8$, as shown in Figs. 4(d) and 5(f). The maximum amplitude record is usually found in the first pick amplitude, for this reason the resulted layer thickness ratios on the first amplitude was chosen to fix the radii of the F^{2}MC tubes, and the radius of layers that gotten from these thickness ratios are detailed in Table 1.

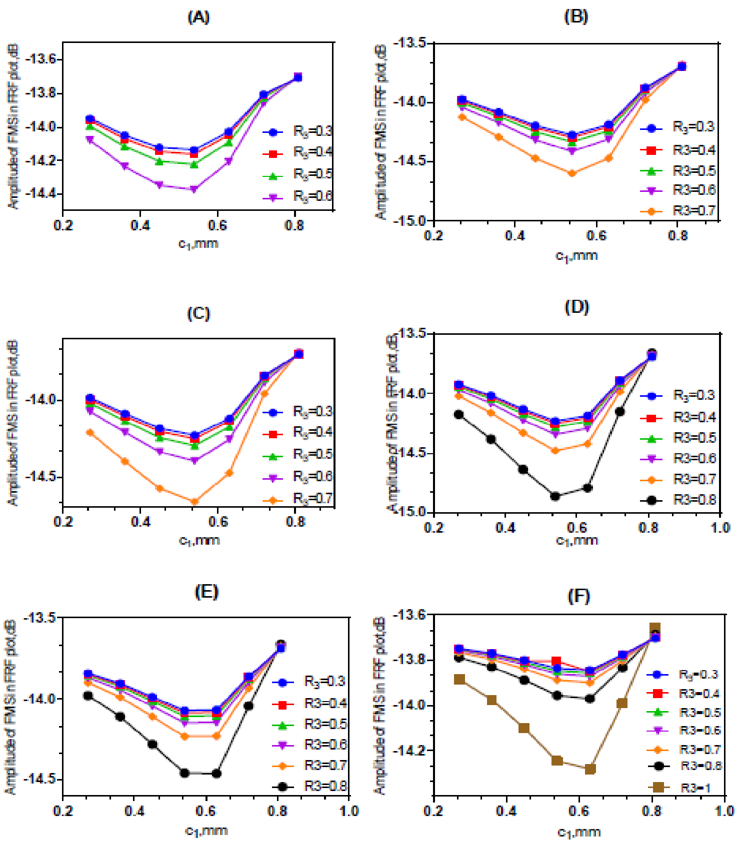

Fig. 4 Optimization result of amplitude of FMS in FRF plot as a function of the tube internal radius c_1 for several values of R_3, and fixed value of c_2 in A, B, C, D, E, and F as 2.25, 1.8, 1.5, 1.28, 1.125, and 1 mm respectively

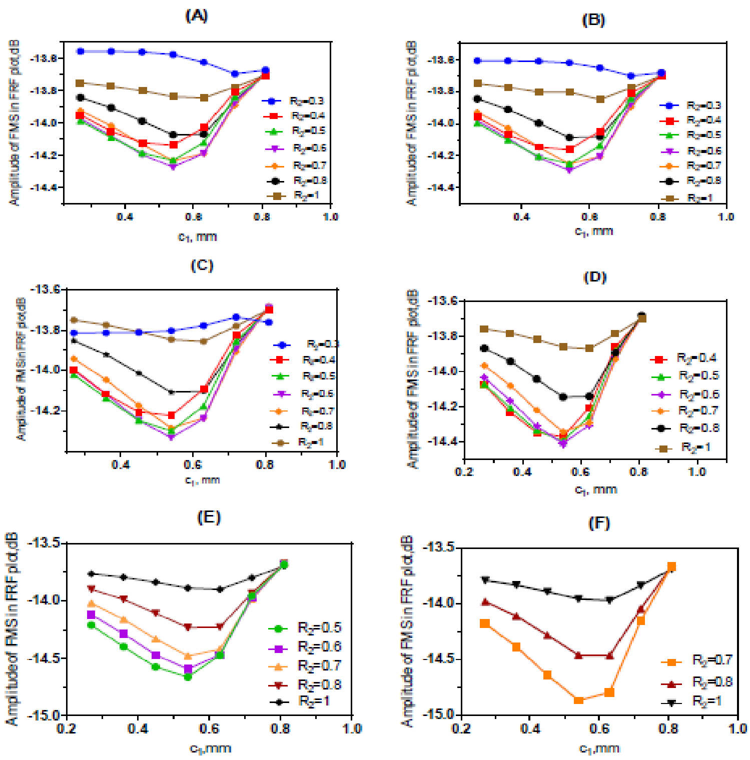

Fig. 5 Optimization result of amplitude of (FMS) in FRF plot as a function of the tube internal radius c_1 for several values of R_2, and fixed value of c_4 in A, B, C, D, E, and F as 10, 5.625, 3.6, 2.5, 1.84, and 1.406 mm respectively

4.2 The selection of points where the tubes are integrated on the beam

In this case various placements from the fixed end to the free end are considered for integration the tubes on the beam. Fig. 6 shows the beam's FRF response with F^{2}MC tubes connected on three different locations on the beam. It can be observed that, placing the tubes on the fixed end of the beam is more effective for damping than other positions, because this position records maximum bending moments. A rose in the system's resonance frequency of 24.54 Hz with a fall of 13 dB in first resonance amplitude can be found if compared with the other bonding positions. In addition, when the second mode shape was taken into account, bonding the tubes on the centre of the beam gives better damping than others, with 8.87 dB lower amplitudes if compared with a clamped end placement. Whilst at same time, placing the tubes on positions with maximum deflection yields the wider cyclic frequency. This result leads to an agreement with the foundations of previous researches (Zhu *et al.* 2015, Miura *et al.* 2015, Krott *et al.* 2015) with better damping efficiency, as the present FMS amplitude is -21.6 dB while (Zhu *et al.* 2015) and (Krott *et al.* 2015) achieved nearly -18, and -17.2 dB reductions in FMS respectively.

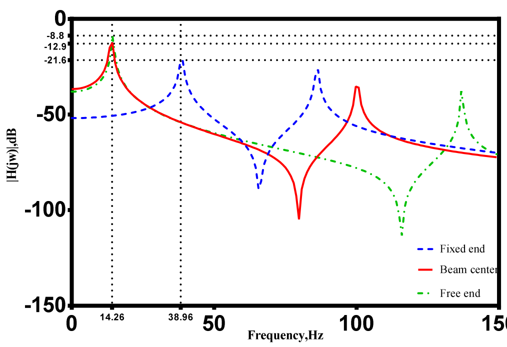

Fig. 6 FRF plot corresponding to 1stand 2nd modes for F^{2}MC tubes integrated on the cantilever beam with different joint placements and $(L_{FMC} = 0.48\text{ L})$; Fixed end (dashed), centre of the beam (solid), and free end (dash-dotted)

4.3 Changing the fluid type

For the F^{2}MC tubes with optimized diameters, length (L_{FMC}), and best bonding location (on the beam's fixed end) several fluids with different bulk moduli, viscosity and density are selected to examine their ability to dissipate the energy that caused by transverse vibrations through beam bending. These fluids were gasoline, water, glycerine and mercury. Their properties explained in Table 2, and the resulted response detailed in Fig. 7. The working fluid has a major role in damping transverse vibrations, because the behaviour of fluidic dampers are usually governed by the speed of fluid flow through the orifices with their mechanical properties (Dalrymple *et al.* 1984). Glycerine is a water-soluble, and viscous liquid. When it was examined as a working media, because of having high viscosity, it increased internal friction with F^{2}MC tube walls, and the viscosity of the fluid is related to fluid drag forces, Chen *et al.* (1976). However, its lost at support points, but this event is small if compared with fluid viscosity effects. The highlights in reductions in resonance frequency by 20.9 Hz and peak amplitude by 3 dB supports the direct relation between fluid viscosity and damping coefficient through comparison with water under the same conditions (Fig. 9). This behaviour was noticed by other researchers (Miller 1965). But both mercury and gasoline recorded similar FMS amplitude with different resonance frequencies. Mercury has the highest bulk modulus, while examining it undamped amplitudes has been obtained. That was because the increase in bulk modulus directly increases fluid's pressure inside the tubes by reducing intermolecular gaps (Temperley and Trevena 1978, Gholizadeh *et al.* 2011). As it might reduce the amount of fluid entering the tubes by beam bending. Some researchers, combine the effect of fluid bulk modulus with F^2MC tubes modulus ratio, and stated that they are directional proportional (Shan *et al.* 2009), and as explained before, damping increases with reducing the modulus ratio. Gasoline is a liquid with lower bulk modulus, and higher viscosity than water, reducing bulk modulus might cause more damping while increasing liquid viscosity more likely to reduce damping. However, the velocity of flow is proportional with mass damping parameter, but it is only influenced in low density fluids like air (Tanaka and Takahara 1981).

Table 7 Properties of selected fluids in this study

Property	Water	Gasoline	Glycerine	Mercury
Bulk Modulus (B_f), GPa	2	1.3	4.35	28.5
Density (ρ_f), Kg/m^3	1000	680	1260	13250
Viscosity (v_f), *Poise*	0.001	0.006	14.9	0.016

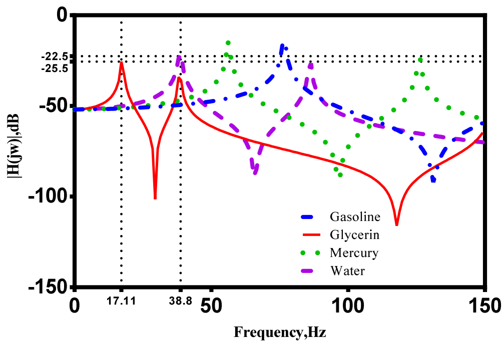

Fig. 7 FRF plot for investigated system F^2MC tubes bonded on the cantilever beam, with different working fluids

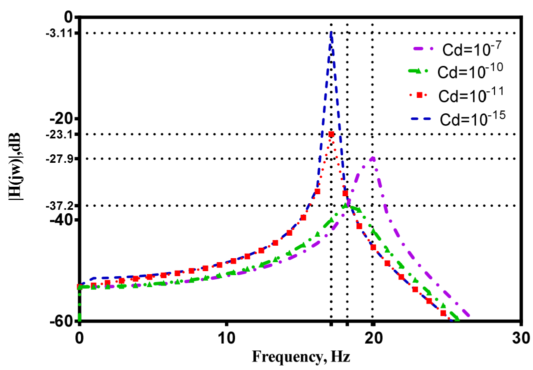

Fig. 8 FRF plot for the system response with different values of flow coefficients C_d (m^3/s pa)

The flow coefficient C_d proposes damping into the system. Fig. 8 shows the frequency response of system with different flow coefficients. As C_d reduced slowly from 10^{-7} – 10^{-10}, the frequency response became more damped, but further reduction in the orifice size ($C_d \approx 0$) prevents the fluid from flowing, undamped peaks are formed. The maximum reduction in first resonance amplitude was near to 23.7 dB with $C_d = 10^{-10}$ m^3/s pa as compared with the system response with $C_d = 10^{-13}$ m^3/s pa (solid plot in Fig. 6).

5. Discussion

In order to compare the analysis results with Literature, the basic material and geometry parameters in the following discussions have fitted the same value as those in the study by Zhu *et al.* (2015). Then the effect of changing the thickness of layers from inside to outside ($R1$, $R2$, and $R3$) for the fixed value of middle layer internal radius ($\boldsymbol{c_2} = \mathbf{0.9\ mm}$) showed that by increasing the inner radius of the tubes until a certain value (0.54 mm) gave more flexibility to the tubes and provided better damping. As it resulted in the increase in internal cavity and more modulus ratio was obtained. Modulus ratio is the ratio of the applied stress to the total amount of strain in the longitudinal direction, (Chen *et al.* 2012). It adds more flexibility to the tubes and provides more damping. With further increase the internal cavity more than this value the first layer thickness is reduced, so the internal volume increased and the fluid inside the tubes expands, so its pressure reduced. In addition to maximizing the modulus ratio by decreasing thickness of inner layer (Shan *et al.* 2009), fewer energy absorbed and larger system vibrations remained. In the same time increasing the middle and outer layer thickness ratios to certain values ($R2$ = 0.7 and $R3$ = 0.8), a reduction in the thickness of these layers due to minimizing their stiffness. Thus, damping is provided. But further increasing due to obtaining very thin layers, so their property as vibration absorbers is going to be lost. Thus, beam vibrations are remained.

Furthermore, by changing the material type of composite fibre reinforced layer, along with using the resulted layer thickness ratios, and comparing the results of the modified diameters with the size selected by literature (Zhu *et al.* 2015), the results showed a decrease in first peak amplitude by 9.15 dB with constant resonance frequency (9). This happened because here the inner, middle and outer layers are thicker by 0.29, 0.55 and 0.24 mm respectively. So, better prevention of fluid leakage to outside is obtained and provides more stiffness (Shan *et al.* 2009). In another side, the decrease of internal cavity of the tubes due to decrease in modulus ratio (Chen *et al.* 2012). The F^2MC tubes with small modulus ratios are stiff tubes, and have smaller longitudinal stains. Regarding to Eqs. (1) and (53), with the beam bending, the tubes are extended, and more

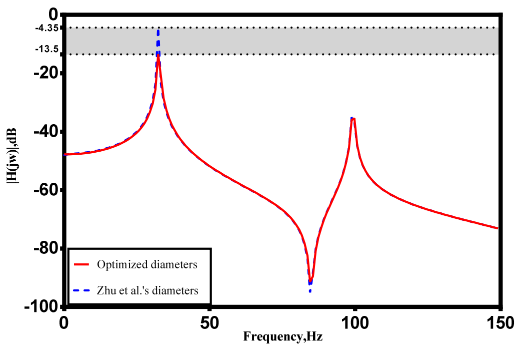

Fig. 9 Comparison in F²MC tube's FRF plot between optimized diameters and the reference's diameters

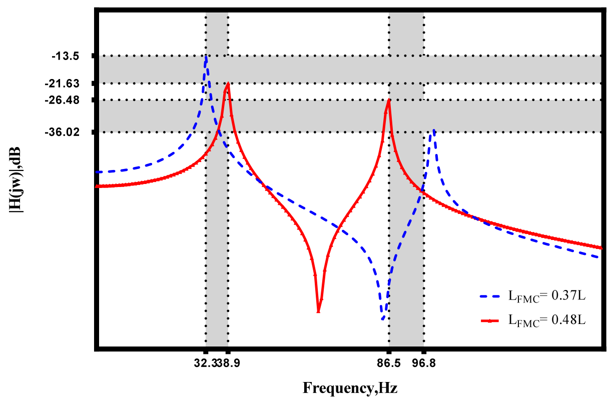

Fig. 10 FRF plot for F²MC tubes placed on the fixed end of the beam with different tube lengths; dotted for $L_{FMC} = 0.37L$ and solid line for $L_{FMC} = 0.48L$

fluid entered into the tubes, fluid pressure inside the tubes is increased thus more damping is achieved. In another words, it can be stated that the tube's modulus ratio is inversely proportional to vibration damping (9). This result is in agreement with findings reported by Philen (2012) which was done on the same tubes for studying vibration isolation, and (Miura *et al.* 2015), which observed the usage of these tubes as high optimal tuning frequency and damping ratio.

The present study selected longer tubes ($L_{FMC} = 0.48L$) if compared with previously done study (Zhu *et al.* 2015). In which the tubes of 115 mm length had been selected, which is nearly $L_{FMC} = 0.37L$. The comparison in magnitude of response between the two tubes integrated on the same beam and under the same conditions highlighted a reduction of 8.12 dB, and 2.59 dB in the first and second resonance amplitudes respectively, with a shift in first and second resonance frequencies by approximately 6, 10 Hz respectively. In Fig. 10, the findings of this study can be supported by results gotten by other researchers (Liu *et al.* 2013).

In the case of changing the fluid type inside the tubes, it can be summarized that, glycerine's efficiency for damping is better than water, it might be considered as the fluid to be used as a working media inside F²MC tubes in different applications. Whereas, neither mercury nor gasoline is recommended as working media inside F²MC tubes, because instead of damping, they recorded higher undamped frequencies by 7.8 dB and 9.41 dB respectively as compared to water under the same conditions. Whereas, reducing flow coefficient to some limit increased the system damping, but further reducing it due to fluid blockage inside the tubes, so F2MC tube's efficiency was reduced.

6. Conclusions

In spite of most recent studies that dealing with vibration control of cantilever structures which focused on active or semi-active vibration control, this study covered a new light on damping treatment of cantilever beams by using passive vibration control. It represents a valuable approach for damping cantilever beam vibrations in a simple way through integration of F²MC tubes on it. During this study the obtained results can be concluded as follow:

(1) The study represented a valuable approach for cantilever beam vibrations through investigations.
(2) The comparison between the results that have been obtained during the analytical study with the experimental study results that was done in Pennsylvania State University, proved the strength and accuracy of the derived model.
(3) The optimizations in layer thickness ratios recorded a reduction of 9.15 dB in First mode shape's amplitude with $R_1 = 0.6$, $R_2 = 0.7$, and $R_3 = 0.8$.
(4) The best bonding position of F²MC tubes on the cantilever beam is with the beginning of the cantilever's clamped end.
(5) Thicker tubes with more flexibility in fiber reinforced layers has been analyzed to obtain more damping.
(6) Glycerin reduced the first resonance amplitude of vibration by 34.34 dB.
(7) A three-layered model of F²MC tubes that composed of two respective fiber reinforced layers was achieved more reductions in resonance amplitude by 12.12 dB.
(8) Installing the patch with the beginning of the fixed end on the beam gives the best performance of the tubes toward damping.
(9) Reducing the fluid's flow coefficient to some limit has positive effect on damping vibrations.

As the results of this study showed an excellent performance of F²MC tubes, they can be applied in real life vibration control applications, especially for applications that require large size F²MC tubes, bubble formulation control must be taken into account, which requires designing a system for reducing the formulation of air bubbles during filling process. because they tend to reduce the damping performance of F²MC tubes system. Applying them as fibres in producing vibration absorber composite sheets. Their high damping performance as absorbers, and isolators makes them efficient enough to be used in vibration control in several applications, such as:

Examining their efficiency in frame works against bomb effects; examining their integration during base construction of multistage buildings. And also, it might give good result in solving the wind caused vibration problems in bridges.

References

Bakaiyan, H., Hosseini, H. and Ameri, E. (2009), "Analysis of multi-layered filament-wound composite pipes under combined internal pressure and thermomechanical loading with thermal variations", *Compos. Struct.*, **88**, 532-541. https://doi.org/10.1016/j.compstruct.2008.05.017

Boresi, A.P., Schmidt, R.J. and Sidebottom, O.M. (1993), *Advanced Mechanics of Materials*, John Willey & Sons Inc., USA.

Casas-Ramos, M.A. and Sandoval-Romero, G.E. (2017), "Cantilever beam vibration sensor based on the axial property of fiber Bragg grating", *Smart Struct. Syst., Int. J.*, **19**(6), 625-631. https://doi.org/10.12989/sss.2017.19.6.625

Chen, S.S., Wambsganss, M.T. and Jendrzejczyk, J.A. (1976), "Added mass and damping of a vibrating rod in confined viscous fluids", *J. Appl. Mech.*, **43**, 325-329.

Chen, Y., Sun, J., Liu, Y. and Leng, J. (2012), "Experiment and analysis of fluidic flexible matrix composite (F^2MC) tube", *J. Intell. Mater. Syst. Struct.*, **23**(3), 279-290. https://doi.org/10.1177/1045389X11420591

Dalrymple, R.A., Kirby, J.T. and Hwang, P.A. (1984), "Wave diffraction due to areas of energy dissipation", *J. Waterway Port Coast. Ocean Eng.*, **110**, 67-69. https://doi.org/10.1061/(ASCE)0733-950X(1984)110:1(67)

Gere, J.M. (2004), *Mechanics of Materials*, Thomson Brooks/Cole.

Ghodsi, M., Ziaiefar, H., Mohammadzaheri, M., Omar, F.K. and Bahadur, I. (2019), "Dynamic analysis and performance optimization of permendur cantilevered energy harvester", *Smart Struct. Syst., Int. J.*, **23**(5), 421-428. https://doi.org/10.12989/sss.2019.23.5.421

Gholizadeh, H., Burton, R. and Schoenau, G. (2011), "Fluid bulk modulus: a literature survey", *Int. J. Fluid Power*, **12**, 5-15. https://doi.org/10.1080/14399776.2011.10781033

Itoh, T., Shimomura, T. and Okubo, H. (2011), "Semi-Active Vibration Control of Smart Structures with Sliding Mode Control", *J. Syst. Des. Dyn.*, **5**, 716-726. https://doi.org/10.1299/jsdd.5.716

Kirn, J., Lorkowski, T. and Baier, H. (2011), "Development of flexible matrix composites (FMC) for fluidic actuators in morphing systems", *Int. J. Struct. Integr.*, **2**, 458-473. https://doi.org/10.1108/17579861111183948

Krott, M.J., Miura, K., LaBarge, S., Rahn, C., Smith, E.C. and Romano, P.Q. (2015), "Tube compliance effects on fluidic flexible matrix composite devices for rotorcraft vibration control", *Proceedings of the 56th AIAA/ASCE/AHS/ASC Structures, Structural Dynamics, and Materials Conference*, Kissimmee, FL, USA.

Kurczewski, N.A., Scarborough III, L.H., Rahn, C.D. and Smith, E.C. (2012), "Coupled Fluidic Vibration Isolators for Rotorcraft Pitch Link Loads Reduction", *International Design Engineering Technical Conferences and Computers and Information in Engineering Conference*, Chicago, IL, USA, pp. 281-281. https://doi.org/10.1115/DETC2012-70174

Lekhnitskii, S.G. (1977), *Theory of Elasticity of an Anisotropic body*, Moscow: Mir Publishers.

Liu, B., Wang, Y.R. and Feng, H.H. (2013), "A Design Method of Position Schemes for Particle Dampers Applied to a Flywheel", *Appl. Mech. Mater.*, **482**, 163-168. https://doi.org/10.4028/www.scientific.net/AMM.482.163

Loktionov, A.P. (2017), "A measuring system for determination of a cantilever beam support moment", Smart Structures and Systems, **19**(4), 431-439. https://doi.org/10.12989/sss.2017.19.4.431

Lotfi-Gaskarimahalle, A., Shan, Y., Li, S., Rahn, C.D., Bakis, C.E. and Wang, K.W. (2008), "Stiffness shaping for zero vibration fluidic flexible matrix composites", *Proceedings of ASME Conference on Smart Materials, Adaptive Structures and Intelligent Systems*, Ellicott, MA, USA. https://doi.org/10.1115/SMASIS2008-501

Lotfi-Gaskarimahalle, A., Scarborough III, L.H., Rahn, C.D. and Smith, E.C. (2009), "Fluidic composite tuned vibration absorbers", *Proceedings of the ASME 2009 Conference on Smart Materials, Adaptive Structures and Intelligent Systems*, Oxnard, CA, USA. https://doi.org/10.1115/SMASIS2009-1349

Miller, R.R. (1965), "The effects of frequency and amplitude of oscillation on the hydrodynamic masses of irregular shaped bodies", University of Rhode Island.

Miura, K., Krott, M., Smith, E., Rahn, C.D. and Romano, P. (2015), "Experimental validation of Tailboom vibration control using fluidic flexible matrix composite tubes", *Proceedings of AHS 71st Annual Forum of the American Helicopter Society*, Virginia Beach, CA, USA, pp. 1252-1260.

Nakahara, T. and Fujimoto, T. (2011), "Energy regenerative active vibration control of cantilever beam using piezoelectric actuator and class d amplifier", *J. Syst. Des. Dy.*, **5**, 737-751. https://doi.org/10.1299/jsdd.5.737

Oueini, S.S., Nayfeh, A.H. and Pratt, J.R. (1998), "A nonlinear vibration absorber for flexible structures", *Nonlinear Dyn.*, **15**, 259-282. https://doi.org/10.1023/A:1008250524547

Philen, M. (2008), "Sliding mode control of variable modulus structures based upon fluidic flexible matrix composites", *49th AIAA/ASME/ASCE/AHS/ASC Structures, Structural Dynamics, and Materials Conference, 16th AIAA/ASME/AHS Adaptive Structures Conference,10th AIAA Non-Deterministic Approaches Conference, 9th AIAA Gossamer Spacecraft Forum, 4th AIAA Multidisciplinary Design Optimization Specialists Conference*, Schaumburg, IL, USA, pp. 1-12. https://doi.org/10.2514/6.2008-2127

Philen, M. (2010), "Tunable modulus structures utilizing fluidic flexible matrix composites: analytical and experimental investigations", *Proceedings of the 51st AIAA/ASME/ASCE/AHS/ASC Structures, Structural Dynamics, and Materials Conference*, Orlando, FL, USA, pp. 2663-2663. https://doi.org/10.2514/6.2010-2663

Philen, M. (2012), "Fluidic flexible matrix composite semi-active vibration isolation mounts", *J. Intell. Mater. Syst. Struct.*, **23**, 353-363. https://doi.org/10.1177/1045389X11421823

Philen, M., Shan, Y., Bakis, C., Wang, K.W. and Rahn, C. (2006), "Variable stiffness adaptive structures utilizing hydraulically pressurized flexible matrix composites with valve control", *Proceedings of the 47th AIAA/ASME/ASCE/AHS/ASC Structures, Structural Dynamics, and Materials Conference*, Newport, RI, USA, pp. 1-11. https://doi.org/10.2514/6.2006-2134

Philen, M.K., Shan, Y., Prakash, P., Wang, K.W., Rahn, C.D., Zydney, A.L. and Bakis, C.E. (2007), "Fibrillar network adaptive structure with ion-transport actuation", *J. Intell. Mater. Syst. Struct.*, **18**, 323-334. https://doi.org/10.1177/1045389X06066097tions

Roberson, R.E. (1952), "Synthesis of a nonlinear dynamic vibration absorber", *J. Franklin Inst.*, **254**, 205-220. https://doi.org/10.1016/0016-0032(52)90457-2

Scarborough, L.H. (2014), "Dynamics of fluidic devices with applications to rotor pitch links", Dissertation; *Pennsylvania State University*, University Park, PA, USA.

Shan, Y., Philen, M.P., Bakis, C.E., Wang, K.W. and Rahn, C.D. (2006), "Nonlinear-elastic finite axisymmetric deformation of flexible matrix composite membranes under internal pressure and axial force", *Compos. Sci. Technol.*, **66**, 3053-3063. https://doi.org/10.1016/j.compscitech.2006.01.002

Shan, Y., Philen, M., Lotfi, A., Li, S., Bakis, C.E., Rahn, C.D. and Wang, K.W. (2009), "Variable stiffness structures utilizing fluidic flexible matrix composites", *J. Intell. Mater. Syst. Struct.*, **20**, 443-456. https://doi.org/10.1177/1045389X08095270

Starosvetsky, Y. and Gendelman, O.V. (2008), "Attractors of harmonically forced linear oscillator with attached nonlinear energy sink. II: Optimization of a nonlinear vibration absorber", *Nonlinear Dyn.*, **51**, 47-57. https://doi.org/10.1007/s11071-006-9168-z

Sun, C.T. and Li, S. (1988), "Three-dimensional effective elastic constants for thick laminates", *J. Compos. Mater.*, **22**, 629-639. https://doi.org/10.1177/002199838802200703

Takács, G., Batista, G., Gulan, M. and Rohal'-Ilkiv, B. (2016), "Embedded explicit model predictive vibration control", *Mechatronics*, **36**, 54-62. https://doi.org/10.1016/j.mechatronics.2016.04.008

Tanaka, H. and Takahara, S. (1981), "Fluid elastic vibration of tube array in cross flow", *J. Sound Vib.*, **77**, 19-37. https://doi.org/10.1016/S0022-460X(81)80005-3

Temperley, H.N.V. and Trevena, D.H. (1978), *Liquids and their Properties: A Molecular and Macroscopic Treatise with Applications*, Bookbarn International, Ellis Horwood Ltd., Bristol, SOM, UK.

Usharani, R., Uma, G., Umapathy, M. and Choi, S.B. (2017), "A new broadband energy harvester using propped cantilever beam with variable overhang", *Smart Struct. Syst., Int. J.*, **19**(5), 567-576. https://doi.org/10.12989/sss.2017.19.5.567

Viguié, R. and Kerschen, G. (2009), "Nonlinear vibration absorber coupled to a nonlinear primary system: a tuning methodology", *J. Sound Vib.*, **326**, 780-793. https://doi.org/10.1016/j.jsv.2009.05.023

Wang, X. and Shi, Z. (2015), "Unified solutions for piezoelectric bilayer cantilevers and solution modifications", *Smart Struct. Syst., Int. J.*, **16**(5), 759-780. https://doi.org/10.12989/sss.2015.16.5.759

Yun, S.K., Yoon, S.S., Kang, S. and Kim, M. (2008), "Design and Vibration Control of Safe Robot Arm with MR-Based Passive Compliant Joint", *J. Syst. Des. Dyn.*, **2**, 475-484. https://doi.org/10.1299/jsdd.2.475

Zhang, Z., Philen, M. and Neu, W. (2010), "A biologically inspired artificial fish using flexible matrix composite actuators: Analysis and experiment", *Smart Mater. Struct.*, **19**, 1-11. https://doi.org/10.1088/0964-1726/19/9/094017

Zhao, Y.Y. and Xu, J. (2007), "Effects of delayed feedback control on nonlinear vibration absorber system", *J. Sound Vib.*, **308**, 212-230. https://doi.org/10.1016/j.jsv.2007.07.041

Zhu, B., Rahn, C.D. and Bakis, C.E. (2011), "Tailored fluidic composites for stiffness or volume change", *Proceedings of Conference on Smart Materials, Adaptive Structures and Intelligent Systems*, Scottsdale, AZ, USA, pp. 607-612. https://doi.org/10.1115/SMASIS2011-4962

Zhu, B., Rahn, C.D. and Bakis, C.E. (2013a), "Vibration damping of a cantilever beam utilizing fluidic flexible matrix composites", *Proceedings of Active and Passive Smart Structures and Integrated Systems*, San Diego, CA, USA, March. https://doi.org/10.1117/12.2014763

Zhu, B., Rahn, C.D. and Bakis, C.E. (2013b), "Vibration damping of a cantilever beam utilizing fluidic flexible matrix composites", *Procedings of Active and Passive Smart Structures and Integrated Systems*, San Diego, CA, USA, March. https://doi.org/10.1117/12.2014763

Zhu, B., Krott, M.J., Rahn, C.D. and Bakis, C.E. (2014a), "Experimental characterization of a cantilever beam with a fluidic flexible matrix composite vibration treatment", *Proceedings of the ASME 2014 International Design Engineering Technical Conferences & Computers and Information in Engineering Buffalo*, New York, USA. https://doi.org/10.1115/DETC2014-34966

Zhu, B., Rahn, C.D. and Bakis, C.E. (2014b), "Fluidic flexible matrix composite vibration absorber for a cantilever beam", *J. Vib. Acoust.*, **137**(2), 021005. https://doi.org/10.1115/1.4029002

Zhu, B., Rahn, C.D. and Bakis, C.E. (2015), "Fluidic flexible matrix composite damping treatment for a cantilever beam", *J. Sound Vib.*, **340**, 80-94. https://doi.org/10.1016/j.jsv.2014.11.042

CC